

Assessment of the mesopore wall catalytic activities of MFI zeolite with mesoporous/microporous hierarchical structures

Vasudev N. Shetti, Jeongnam Kim, Rajendra Srivastava, Minkee Choi, Ryong Ryoo *

Center for Functional Nanomaterials and Department of Chemistry, Korea Advanced Institute of Science and Technology, Daejeon 305-701, Republic of Korea

Received 7 October 2007; revised 24 December 2007; accepted 2 January 2008

Available online 1 February 2008

Abstract

MFI zeolite with a mesoporous/microporous hierarchical structure (MeMFI zeolite) was hydrothermally synthesized with an organosilane surfactant. The acid catalytic activities of the mesopore walls were evaluated for various reactions involving bulky molecules, such as the protection of benzaldehyde with pentaerythritol, the condensation of benzaldehyde with 2-hydroxyacetophenone, the esterification of benzylalcohol with hexanoic acid, and the cracking of branched polyethylene. The catalytic activities of pristine MeMFI zeolite were very high compared with those of a conventional MFI catalyst. The catalytic activities of MeMFI were lost almost completely after selective dealumination of the surface Al on the mesopore walls using tartaric acid. For small molecular reactions, however, the mesoporous zeolite still exhibited high catalytic activities even after the dealumination process. This indicates that bulky molecular reactions occurred due to Al sites located at the surface of the mesopore walls. © 2008 Elsevier Inc. All rights reserved.

Keywords: Mesoporous zeolite; Hierarchical zeolite; Acidity; Dealumination; Bulky molecular reactions; Catalytic activity

1. Introduction

Crystalline microporous zeolites find extensive applications as acid catalysts in the petrochemical and in fine chemical syntheses due to their high ion-exchange capacity, strong acidity, high stability, and shape selectivity. Despite these advantages, the catalytic applications of zeolite are limited by slow diffusion into the micropores when reactions of bulky molecules are concerned. Ordered mesoporous aluminosilicates with various structures [1–4] were synthesized to solve the diffusion limitation of zeolites. Due to an amorphous framework, however, the MCM-41-like mesoporous materials exhibited lower hydrothermal stability, weaker acidity, and lower catalytic activities than their zeolite counterparts [5–8].

Considerable efforts have been devoted to the development of mesoporous materials that have a zeolitic framework, with the aim of combining the advantages of the high acidity of the crystalline zeolite and the facile diffusion of bulky molecules in a mesoporous material. In a previous approach, sur-

factants were added to the zeolite synthesis composition in an attempt to generate mesoporosity in the zeolite crystals [9,10]; however, this approach gave a physical mixture of ordinary zeolite and mesoporous material with an amorphous framework. Another strategy was to synthesize mesoporous materials by assembling presynthesized zeolite seeds in the presence of surfactants [11]. The resultant materials exhibited a significant increase in their acid catalytic activities compared with the aforementioned MCM-41-type materials; however, the structure of the framework did not demonstrate zeolite crystallinity. A third approach was to perform zeolite crystallization within the matrix of presynthesized “rigid” nanotemplates (e.g., carbon nanoparticles [12], nanofibers [13], mesoporous carbon [14], or polymer beads [15]), followed by template removal through calcination. This method successfully generated mesoporous materials with highly crystalline zeolite walls, although the tunability of the mesopore structure was limited by the availability of templates. Choi et al. [16] developed a different strategy for the direct synthesis of zeolite with tunable mesoporosity using organosilane surfactants as a mesopore director. The resultant zeolites were highly mesoporous, and the mesopore walls showed characteristics of a fully crystalline zeolite framework. The mesopore diameters were tunable by

* Corresponding author. Fax: +82 42 869 8130.
E-mail address: ryoo@kaist.ac.kr (R. Ryoo).

the chain length of the surfactants. Recently, nonamphiphilic organosilane [17], silylated polymer [18], and cationic polymers [19] have been used to synthesize mesoporous zeolites.

Srivastava et al. [20] recently reported that MFI zeolite with a mesoporous/microporous hierarchical structure (MeMFI zeolite) showed remarkably improved resistance to the deactivation of the catalytic activities in various reactions involving small molecules. In addition, the MeMFI zeolite exhibited very high catalytic activity in the synthesis of jasminaldehyde (α -*n*-amylcinnamaldehyde) and vesidryl (2',4,4'-trimethoxychalcone). The high activities in the reactions of such bulky molecules indicate that MeMFI zeolite is a promising catalyst for the reactions of bulky molecules requiring mild acidity. However, the catalytic properties of MeMFI in reactions requiring stronger acidity (e.g., esterification and cracking) have not yet been investigated.

In the present work, we systematically characterized the surface acidic sites in mesoporous zeolites by carrying out various reactions of bulky molecules before and after selective surface dealumination using L-tartaric acid [21]. The catalytic properties of MeMFI were measured in the protection of benzaldehyde with pentaerythritol, condensation of 2-hydroxyacetophenone with benzaldehyde, esterification of hexanoic acid with benzyl alcohol, and cracking of branched polyethylene (PE). The acidity, and hence the activity, of the surface Al in the mesoporous zeolite were analyzed and compared with those of mesoporous aluminosilicate Al-MCM-41 and conventional MFI zeolite (CoMFI).

2. Experimental

2.1. Preparation of catalyst

MeMFI zeolite was hydrothermally synthesized with [3-(trimethoxysilyl)propyl] dodecyldimethylammonium chloride (TPDAC) as a mesopore-directing agent, after modifying a previously reported synthesis procedure [16]. The procedure was modified to use water glass (a sodium silicate solution) instead of tetraethoxysilane. In the modified synthesis procedure, 4.01 g of TPDAC (51.45 wt% methanol solution), 2.66 g of tetrapropylammonium bromide (TPABr), and 0.77 g of NaOH were completely dissolved in 36.3 g of H₂O and mixed with 83.3 g of diluted sodium silicate solution (Si/Na = 1.75; 6.83 wt% SiO₂). A solution containing 0.48 g of sodium aluminate (53 wt% Al₂O₃, 43 wt% Na₂O; Riedel–deHaën) and 26.6 g of H₂O was added dropwise under stirring to the resultant mixture. Subsequently, 26 g of 10 wt% H₂SO₄ solution was added to the synthesis mixture under vigorous stirring. The final molar composition of the mixture was 2.5 Al₂O₃/40 Na₂O/95 SiO₂/10 TPABr/26 H₂SO₄/9000 H₂O/5 TPDAC. The mixture was heated under stirring at 423 K for 4 days in a Teflon-coated stainless steel autoclave. The precipitated product was filtered by suction and washed with distilled water. The sample was then washed with methanol under refluxing for 12 h to remove traces of physically occluded silane surfactants. The product was dried in an oven at 373 K and subsequently calcined in air at 823 K. The sample was ion-exchanged into the NH₄⁺ form by

repeating the ion-exchange treatment three times with a 1 mol aqueous solution of NH₄NO₃ at 353 K for 4 h. The zeolite was calcined at 823 K for 6 h to convert it to the H⁺ form. CoMFI zeolite was synthesized at 423 K using the same synthesis composition as for MeMFI, but without the silane surfactant. An MCM-41 sample containing Al (Al-MCM-41) was prepared as reported previously [22].

The TPDAC organosilane surfactant was synthesized as described previously [16]. TPDAC may be substituted with dimethyloctadecyl [3-(trimethoxysilyl)propyl] ammonium chloride, which is commercially available (Acros).

Dealumination of CoMFI and MeMFI was performed using L-tartaric acid [21]. The experimental conditions were optimized so that Al could be completely removed from the mesopore walls, but not substantially from the zeolite micropores. In a typical experiment, 1 g of sample was stirred with 20 mL of aqueous L-tartaric acid solution (1 mol) at 353 K for 4 h. The acid treatment was repeated three times to ensure complete dealumination from the surface of the mesopore walls. The dealuminated CoMFI and MeMFI zeolites are designated CoMFI-deAl and MeMFI-deAl, respectively.

2.2. Characterization of the materials

X-ray diffraction (XRD) patterns were recorded with a Rigaku Multiflex diffractometer equipped with CuK α radiation (40 kV, 40 mA). Nitrogen adsorption–desorption isotherms were measured at 77 K using a Quantachrome AS-1MP volumetric adsorption analyzer. Before the measurements, the samples were evacuated for 12 h at 623 K. The Brunauer–Emmett–Teller (BET) equation was used to calculate the apparent surface area from the adsorption data obtained at P/P_0 between 0.05 and 0.2. The pore size distribution was calculated by the Barrett–Joyner–Halenda (BJH) method using the adsorption branch.

Scanning electron microscopy (SEM) was performed with a Hitachi S-4800 microscope operating at 2 kV without metal coating [23]. Solid-state ²⁷Al MAS-NMR spectra were recorded in the fully hydrated state on a Bruker AM-300 NMR spectrometer, using a 7-mm MAS probe. The typical spinning rate was 4 kHz. ²⁷Al MAS-NMR spectra were acquired with 0.5 s repetition time, 3 μ s delay time, and 2000 scans. The chemical shift was referenced to a 1-mol aqueous Al(NO₃)₃ solution.

Elemental analyses were performed by inductively coupled plasma–atomic emission spectroscopy (ICP–AES) using an OPTIMA 4300 DV (Perkin–Elmer). The solution for the ICP–AES analysis was prepared by digesting ca. 0.1 g of zeolite powder in a solution obtained by mixing 1 mL of 36 wt% HCl, 0.5 mL of 50 wt% HF, 1 mL of 63 wt% HNO₃, and 4 mL of H₂O. After digestion, HF was neutralized with 2 g of boric acid. The final solution was diluted with distilled water to the desired concentration (approximately 1000 ppm).

The acidity of the surface Al was measured by a gravimetric method using 2,6-di-*tert*-butylpyridine (DTBPy) as a probe molecule. The gravimetric adsorption measurement of DTBPy was performed using a high-accuracy magnetic suspension balance (Rubotherm; sensitivity, 0.01 mg). DTBPy was used as

received from TCI. Before adsorption, the sample was evacuated for 8 h at 673 K. After being cooled to 298 K, the sample was allowed to adsorb DTBPy at 10^{-3} Pa for 10 h, and then was evacuated at 393 K for 4 h to remove physisorbed DTBPy. The weight of the sample was recorded after cooling to 298 K.

2.3. Catalytic experiments

2.3.1. Reagents

Benzyl alcohol, hexanoic acid, hexadecane, pentaerythritol, benzaldehyde, cyclohexanone, methanol, 2-hydroxyacetophenone, and PE (ultra-high molecular weight; 95%) were received from Sigma Aldrich and used without further purification.

2.3.2. Protection of benzaldehyde with pentaerythritol

The reaction was carried out using a Pyrex batch reactor (EYELA chemistation) equipped with a reflux condenser [20]. Typically, 1.06 g of benzaldehyde (10 mmol), 0.681 g of pentaerythritol (5 mmol), 4 mL of toluene, and 20 mg of freshly activated catalyst were placed into the glass reactor and heated under stirring for 2 h at 393 K. After being cooled to room temperature, the reaction mixture was diluted with 2 mL of 1,2-dichloroethane. The diluted samples were analyzed on a gas chromatograph (Hewlett–Packard 5890 Series II) equipped with a flame ionization detector and a packed column with 10% SE-30.

2.3.3. Condensation of 2-hydroxyacetophenone with benzaldehyde

A reaction mixture containing benzaldehyde (0.75 g, 7 mmol) and 2-hydroxyacetophenone (0.476 g, 3.5 mmol) with 50 mg of catalyst was heated under stirring for 8 h at 423 K in the same Pyrex reactor used in the reaction of benzaldehyde with pentaerythritol. After the reaction, the mixture was cooled and diluted with 3 mL of acetone, to ensure product dissolution before GC analysis. The GC analysis was performed as described above.

2.3.4. Esterification of benzyl alcohol with hexanoic acid

The Pyrex reactor was charged with hexanoic acid (0.58 g, 5 mmol), benzyl alcohol (0.54 g, 5 mmol), 1.8 g of toluene solvent, 50 mg of catalyst, and 0.1 g of hexadecane (internal standard for GC analysis). The reaction was carried out under stirring at 403 K for 4 h. Products were analyzed by GC.

2.3.5. Cracking of branched PE

The reaction was performed in a specially designed Pyrex batch reactor fitted with an overhead stirrer [24]. First, 10 g of PE was placed in the reactor and melted at 623 K. After the addition of 0.1 g of catalyst, the reactor temperature was further increased to 653 K. N_2 gas was passed into the reactor at a rate of 40 mL min^{-1} . The stirring rate was 100 rpm. The reaction was performed at 653 K for 0.5 h. The reaction yield was calculated from the mass change during the reaction.

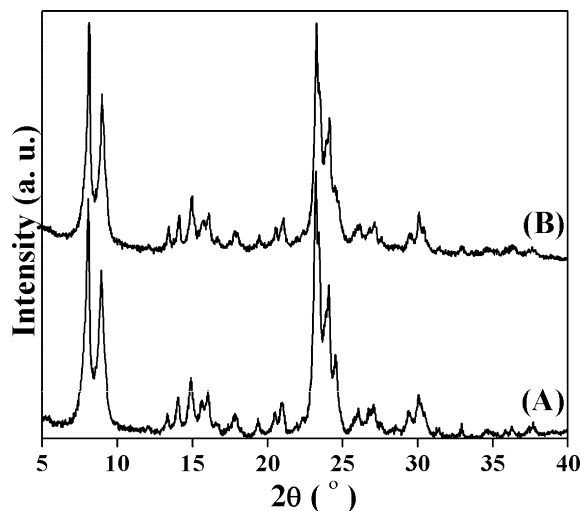


Fig. 1. Powder XRD patterns of mesoporous MFI zeolites: (A) pristine sample (MeMFI), and (B) dealuminated sample with L-tartaric acid (MeMFI-deAl).

2.3.6. *O*-Methylation of cyclohexanone

Cyclohexanone (0.98 g, 10 mmol) and methanol (3.2 g, 100 mmol) were charged with 0.1 g of catalyst in a 20-mL Pyrex vial. The reaction was carried out at 298 K for 2 h under magnetic stirring.

3. Results and discussion

3.1. Material characterization

The XRD pattern of MeMFI revealed that the zeolite was highly crystalline with a MFI topology (Fig. 1A). The dealuminated zeolite, MeMFI-deAl, also exhibited an XRD pattern corresponding to a highly crystalline MFI structure (Fig. 1B). Nitrogen adsorption–desorption isotherms of the MeMFI and MeMFI-deAl zeolite showed type-IV isotherms with sharp condensation in the range of $P/P_0 = 0.8–0.9$, due to the capillary condensation in open mesopores (Fig. 2). Table 1 gives the pore volume, BET area, and Al content of the zeolite samples. The MeMFI zeolite showed much higher specific surface area and pore volume ($570 \text{ m}^2 \text{ g}^{-1}$ and 0.7 mL g^{-1}) compared with CoMFI ($326 \text{ m}^2 \text{ g}^{-1}$ and 0.18 mL g^{-1}). The higher specific surface area and larger pore volume of MeMFI can be attributed to the formation of mesopores. Fig. 3 shows that the MeMFI zeolite particles were composed of nanosized zeolite frameworks. The framework thickness ranged from 8 to 16 nm, according to an analysis of the nitrogen adsorption isotherm of its carbon replica [25]. Compared with MeMFI, the CoMFI sample showed much thicker crystals ($>30 \text{ nm}$); see the SEM images in Fig. 3.

There were no significant decreases in the surface area and pore volume of MeMFI due to dealumination with L-tartaric acid. The ICP-AES analysis data showed that the same treatment with L-tartaric acid led to the removal of 64% of the Al from MeMFI and 21% of the Al from CoMFI. This significant difference can be attributed to the large difference in the external surface areas of the samples. Dealumination should occur rapidly from the external surface of the zeolite particles

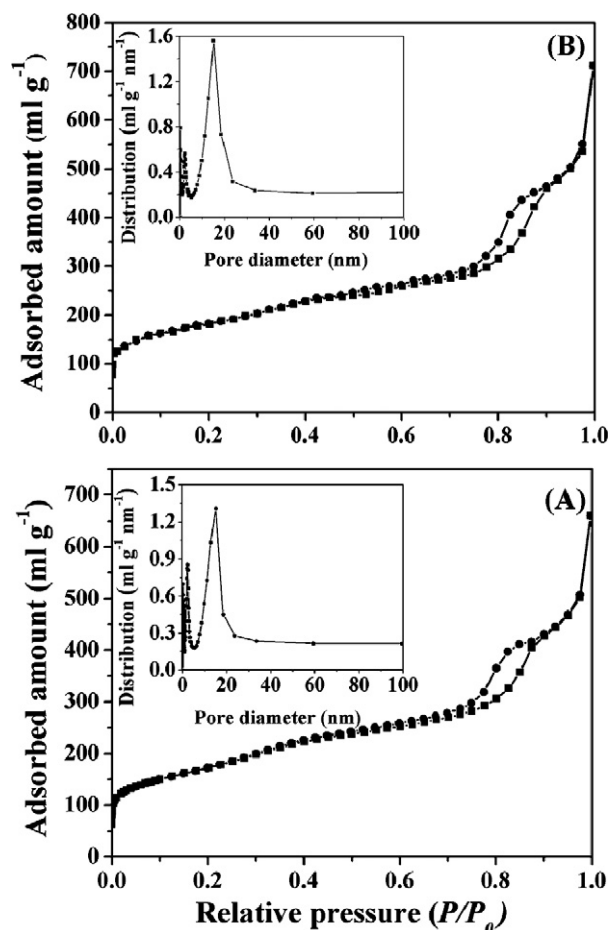


Fig. 2. N_2 adsorption isotherms and pore size distributions (obtained by BJH method using the adsorption branch) of mesoporous MFI zeolites: (A) pristine sample (MeMFI), and (B) dealuminated with L-tartaric acid (MeMFI-deAl).

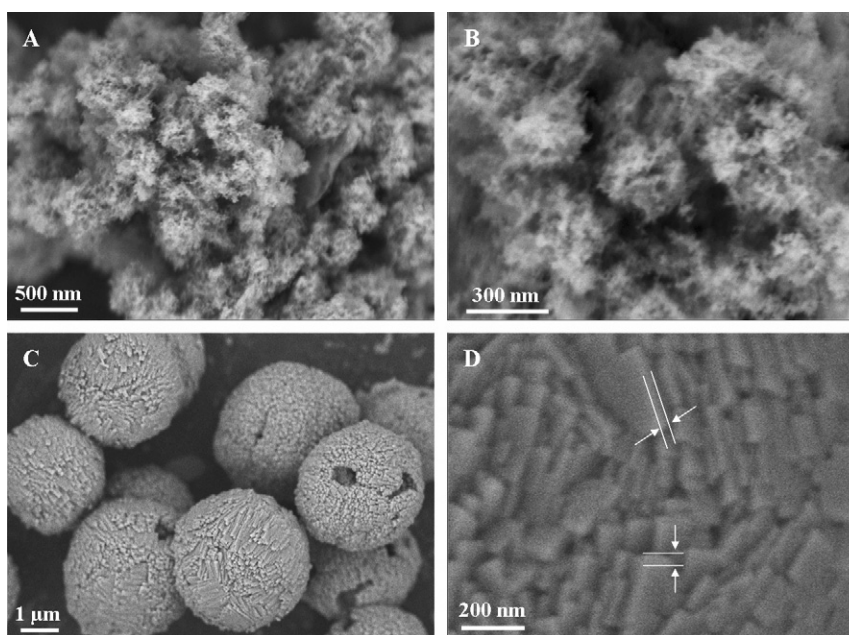


Fig. 3. SEM images of MFI zeolites: (A, B) mesoporous zeolite (MeMFI), and (C, D) zeolite synthesized according to conventional procedure (CoMFI). White parallel lines indicate the crystal thickness.

Table 1
Physico-chemical properties of porous materials used as catalysts

Catalyst	Si/Al ^a	S_{BET} ^b ($m^2 g^{-1}$)	V_p ^c ($mL g^{-1}$)	External Al ^d ($\mu mol g_{cat}^{-1}$)	Total Al ^e ($\mu mol g_{cat}^{-1}$)
MeMFI	17	570	0.70	234	955
MeMFI-deAl	49	575	0.73	14.7	343
Al-MCM-41	20	930	0.69	560	833
CoMFI	26	326	0.18	38.1	635
CoMFI-deAl	33	342	0.17	20.5	505

^a Obtained from ICP-AES analysis.

^b Specific BET surface area obtained from N_2 adsorption isotherms.

^c Total pore volume obtained at $P/P_0 = 0.95$.

^d Calculated by gravimetric measurement of chemisorption of 2,6-di-*tert*-butylpyridine.

^e Obtained from ICP analysis.

but much more slowly from the internal framework, due to the diffusion limitation of tartaric acid. The micropore diameter of MFI zeolite (~ 0.55 nm) is smaller than the kinetic diameter of tartaric acid molecules (0.68 nm). Thus, it is reasonable that the dealumination rate of MeMFI is faster than that of CoMFI.

Basic organic amines can be adsorbed at the acidic Al sites in zeolite. In the case of DTBPy, the molecule is too bulky (0.8 nm diameter) to enter the 10-membered ring systems of the ZSM-5 framework [26,27]. Therefore, it may be assumed that DTBPy can be adsorbed only on Al sites at the external surface (or the surface of the mesopore walls). Considering the molecular size, it is also reasonable to assume that no more than one DTBPy molecule can be adsorbed per Al site. Based on these assumptions, the adsorption of DTBPy over the MeMFI zeolite can be ascribed to the acid site density at the surface of the mesopore walls. The external Al concentration of MeMFI thus determined was $234 \mu mol g^{-1}$ (Table 1). On the other hand, the ICP-AES analysis revealed a total Al concentration of $955 \mu mol g^{-1}$. The difference between these two values can be considered the in-

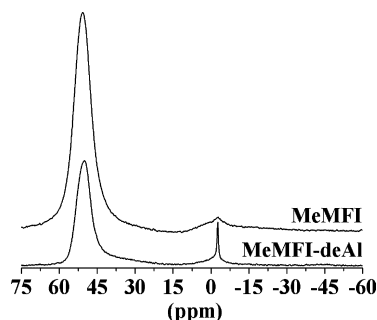


Fig. 4. ^{27}Al -NMR spectra of mesoporous MFI zeolites: pristine sample (MeMFI) and dealuminated sample with L-tartaric acid (MeMFI-deAl). The NMR spectra are compared in the same intensity scale, after the same number of acquisitions under the same conditions.

Table 2

Catalytic data of the catalysts in liquid phase protection of benzaldehyde by pentaerythritol^a

Catalyst	Conv. of benzaldehyde (mol%)	Product selectivity (mol%)	
		Diacetal	Monoacetal
MeMFI	100	95	5.0
MeMFI-deAl	0.7	100	0.0
Al-MCM-41	95	100	0.0
CoMFI	0.0	–	–
CoMFI-deAl	0.0	–	–

^a Reaction conditions: Benzaldehyde (10 mmol), pentaerythritol (5 mmol), toluene (4 mL), catalyst 0.02 g, temperature 393 K, reaction time 2 h.

ternal Al sites that were inaccessible to DTBPy. Table 1 shows that the external Al concentration of the mesoporous zeolite decreased from 234 to 14.7 $\mu\text{mol g}^{-1}$, due to dealumination with tartaric acid. In the case of the CoMFI zeolite, the acid sites were mostly located at the internal surface, where DTBPy was not accessible. The external Al concentration was very low (38.1 $\mu\text{mol g}^{-1}$), as shown in Table 1.

Fig. 4 shows ^{27}Al MAS-NMR spectra of MeMFI and MeMFI-deAl in a fully rehydrated state after calcination at 823 K. The NMR spectra show two peaks. The intense peak at ~ 55 ppm is the tetrahedral Al signal. The second peak appearing at ~ 0 ppm with lower intensity can be assigned to the octahedral Al in the form of polymeric oxo-hydroxo-Al-cations [28] and can be ascribed to the extra-framework Al species [29] or the framework Al species located at the defect sites [30]. The ^{27}Al MAS-NMR spectrum of MeMFI-deAl shows a considerably decreased intensity of the 55-ppm signal. The dealumination also resulted in peak narrowing at ~ 0 ppm. This result is in accordance with removal of the framework Al by tartaric acid; however, it is noteworthy that the octahedral Al species did not completely disappear even after the dealumination treatment.

3.2. Catalytic activity

3.2.1. Activity of the external surface Al sites for bulky molecular reactions

Tables 2–4 summarize the catalytic activities for the protection of benzaldehyde with pentaerythritol, condensation of

Table 3

Catalytic data of the catalysts during condensation of 2-hydroxyacetophenone with benzaldehyde^a

Catalyst	Conv. of 2-hydroxyacetophenone (mol%)	Product selectivity (mol%)		
		Flavonone	Chalcone	Others
MeMFI	82	61	23	16
MeMFI-deAl	0.8	100	0.0	0.0
Al-MCM-41	55	55	27	18
CoMFI	8.4	69	31	0.0
CoMFI-deAl	0.0	–	–	–

^a Reaction conditions: Benzaldehyde (7 mmol), 2-hydroxyacetophenone (3.5 mmol), catalyst 0.05 g, temperature 423 K, reaction time 8 h.

Table 4

Catalytic data of the catalysts in liquid phase esterification of hexanoic acid with benzyl alcohol^a

Catalyst	Conv. of hexanoic acid (mol%)	Product selectivity (mol%)	
		Benzylhexanoate	Dibenzyl ether
MeMFI	75	79	21
MeMFI-1st recycle	71	76	24
MeMFI-2nd recycle	71	77	23
MeMFI-deAl	4.2	100	0.0
Al-MCM-41	21	71	29
CoMFI	4.5	100	0.0
CoMFI-deAl	3.8	100	0.0

^a Reaction conditions: Hexanoic acid (5 mmol), benzyl alcohol (5 mmol), toluene (2 mL), hexadecane (internal standard; 0.44 mmol), catalyst 0.05 g, temperature 403 K, reaction time 4 h.

Table 5

Catalytic data of the catalysts during cracking of branched PE into volatile products^a

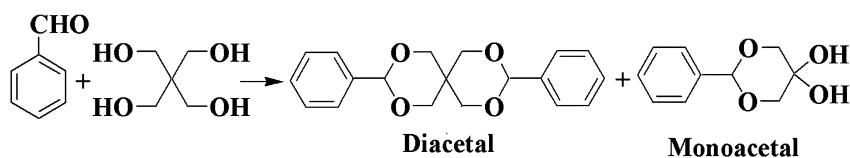
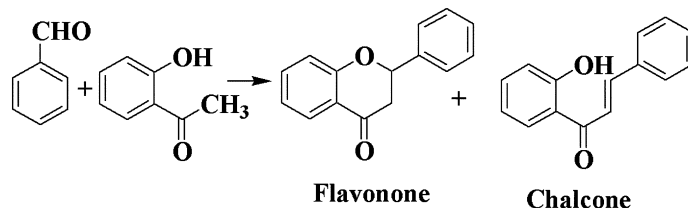
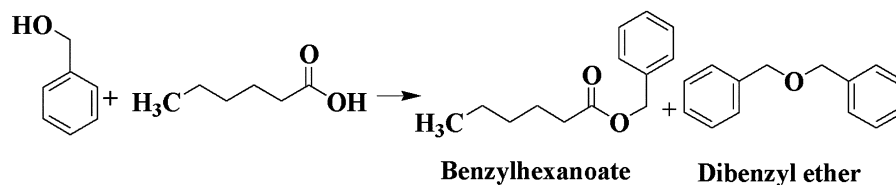
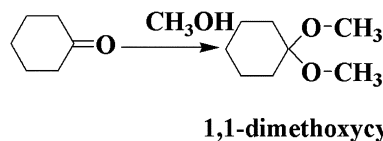
Catalyst	Conv. of branched PE ^b (%)
No catalyst	1.9
MeMFI	88.2
MeMFI-deAl	12.4
Al-MCM-41	8.8
CoMFI	10.4
CoMFI-deAl	8.2

^a Reaction conditions: Branched PE (10 g), catalyst 0.1 g, N_2 flow 40 mL min^{-1} , temperature 653 K, reaction time 30 min.

^b Calculated from the mass balance of PE before and after the reaction.

2-hydroxyacetophenone with benzaldehyde, and esterification of benzyl alcohol with hexanoic acid (Scheme 1). These reactions of bulky molecules were investigated because of their practical applications. Pentaerythritol acetals are used as plasticizers or vulcanizers, as physiologically active substances, and as a protective group for aldehydes or ketones during organic reactions [31]. Flavonoids have found a wide range of applications, including UV protection, flower coloration, interspecies interaction, and plant defense; they also offer nutritional and medicinal values to humans [32]. The low-cost synthesis of bulky ester molecules is an important reaction in the fragrance industries.

Catalytic cracking of branched PE (Table 5) was chosen to investigate whether MeMFI also could have sufficient catalytic activity for cracking reactions, which require stronger acidity

(1) Protection of benzaldehyde with pentaerythritol**(2) Condensation of benzaldehyde with 2-hydroxyacetophenone****(3) Esterification of benzylalcohol with hexanoic acid****(4) O-methylation of cyclohexanone with methanol**

Scheme 1. Organic reactions carried out in the present study.

than the aforementioned reactions. Except for the cracking reaction, both MeMFI and Al-MCM-41 exhibited higher activities compared with CoMFI. The low activities of CoMFI can be attributed to a diffusion limitation due to its small pore diameter. The high catalytic activities of MeMFI indicate that the reactions were catalyzed at the surface of the mesopore walls. Because the condensation and esterification reactions are catalyzed by Brønsted acids, the active sites can be assigned to the framework tetrahedral Al species, where the trivalent cation (i.e., Al³⁺) along with proton (H⁺) act as Brønsted acid sites. For the cracking reaction, the activities increased in the order Al-MCM-41 < CoMFI ≪ MeMFI (Table 5). The MeMFI catalyst exhibited the highest activity due to its high concentration of external Al with high turnover frequency.

The MeMFI zeolite exhibited similar activity to Al-MCM-41 for the aldol condensation reaction of benzaldehyde with pentaerythritol (Table 2). However, in the Claisen–Schmidt condensation of benzaldehyde with 2-hydroxyacetophenone, MeMFI exhibited a slightly higher conversion rate than Al-MCM-41 (Table 3). It is worth noting that the hierarchical mesoporous/microporous material (MeMFI) displayed stronger acidity than Al-MCM-41 [16]. From these results, it can be inferred that the condensation reactions occur at the surface Al species irrespective of their acidic strength.

Table 6

Catalytic data of the catalysts in O-methylation of cyclohexanone^a

Catalyst	Conv. of cyclohexanone (mol%) ^b
MeMFI	74
MeMFI-deAl	71
Al-MCM-41	64
CoMFI	74
CoMFI-deAl	73

^a Reaction conditions: Cyclohexanone (10 mmol), methanol (100 mmol), catalyst 0.1 g, temperature 298 K, reaction time 2 h.

^b The product formed is 1,1-dimethoxycyclohexane with selectivity ca. 100%.

3.2.2. Effect of dealumination from the external surface

In contrast to the high catalytic activity of MeMFI, the MeMFI-deAl zeolite exhibited very low catalytic activity for the aforementioned reactions involving bulky molecules (Tables 2–5). Thus, on dealumination with L-tartaric acid, the mesoporous zeolite lost almost all of its catalytic activity for large molecular reactions. In the O-methylation of cyclohexanone, however, no significant changes in catalytic activity occurred (Table 6), probably due to the small molecular size of the reagents. As discussed in Section 3.1, the treatment with tartaric acid removed the external Al species (changed from

234 to 15 $\mu\text{mol g}^{-1}$); nevertheless, 36% of the initial Al content remained (343 vs 955 $\mu\text{mol g}^{-1}$). The remaining Al can be attributed to the internal acid sites. These Al sites are responsible for the O-methylation of cyclohexanone, where methanol is activated by the internal Al sites. The conversion of cyclohexanone was negligible in the absence of MeMFI or MeMFI-deAl under the present reaction conditions. It is noteworthy that MeMFI-deAl showed comparable catalytic activity to MeMFI even though it had a lower Al concentration. This phenomenon may be ascribed to the compensation effect between acidity enhancement of individual Al sites and Al loss. Indeed, the O-methylation reaction depended on the acidic strength [33]. The catalytic reaction data reported here support the finding that the aforementioned reactions of bulky molecules were catalyzed by the external surface Al of the MeMFI zeolite.

3.2.3. Esterification and cracking reactions occurring at the mesopore walls

Despite the apparently lower Al abundance at the external surface (234 $\mu\text{mol g}^{-1}$ in MeMFI vs 560 $\mu\text{mol g}^{-1}$ in Al-MCM-41), MeMFI revealed a much higher catalytic activity during esterification of benzyl alcohol with hexanoic acid compared with Al-MCM-41 (Table 4). It is noteworthy that small organic acids can catalyze esterification reactions as a Brønsted acid, because they can be easily ionized in water, which is liberated during the reaction. However, bulky organic acids, such as that used here, do not self-catalyze the reaction, because of their low solubility in water. Esterification of such bulky molecules requires a catalyst with high acidity. Therefore, the high catalytic activity of MeMFI indicates that the MeMFI zeolite is a much more active catalyst than Al-MCM-41. A recycling test for MeMFI was carried out to confirm the durability of zeolite catalyst during the esterification reaction. After each reaction, the catalyst was collected and regenerated by calcination at 823 K for 4 h. Subsequent runs demonstrated no significant decreases in the catalytic properties (Table 4).

Catalytic cracking of PE is a reaction requiring much stronger acidity than the esterification reaction discussed above. The C–C chain branching makes the cracking reaction more difficult than in linear PE. Although Al-MCM-41 is known to crack low-density PE, its acidity is reportedly insufficient to crack high-density PE [34]. However, the results presented in Table 5 show that the MeMFI zeolite can crack branched PE, with 88% conversion obtained within 30 min of reaction and almost complete cracking within 1 h of reaction. The catalytic activity of the MeMFI zeolite was many times greater than that of Al-MCM-41 (8.8% conversion at 30 min). This indicates that the surface acidity of MeMFI was indeed much higher than that of Al-MCM-41. Also note that the catalytic conversion was very low in CoMFI, because the conventional MFI zeolite had a very low external surface area and, accordingly, a low concentration of external Al (Table 1).

4. Conclusion

The MeMFI zeolite investigated in the present work has a mesoporous/microporous hierarchical structure. This zeolite

exhibited good catalytic activity in reactions of bulky molecules, including the protection of benzaldehyde with pentaerythritol, condensation of benzaldehyde with 2-hydroxyacetophenone, esterification of benzylalcohol with hexanoic acid, and cracking of branched PE, which could not occur inside the MFI zeolite micropores. After the selective dealumination of the external Al species using tartaric acid, the zeolite became catalytically inactive for these reactions. The results clearly indicate that the catalytic reactions occurred at the acidic Al sites on the mesopore walls of the MeMFI zeolite. These catalytic activities were correlated with the number of Al sites located at the mesopore walls, which was determined by the chemisorption of 2,6-di-*tert*-butylpyridine. In conclusion, mesoporous zeolite has been found to be a versatile acidic catalyst for a range of bulky molecular reactions requiring both mild and strong acidity.

Acknowledgments

This work was supported in part by the National Honor Scientist Program of the Korean Ministry of Science and Technology and by the School of Molecular Science through the Brain Korea 21 Project.

References

- [1] C.T. Kresge, M.E. Leonowicz, W.J. Roth, J.C. Vartuli, J.S. Beck, *Nature* 359 (1992) 710.
- [2] D. Zhao, J. Feng, Q. Huo, N. Melosh, G.H. Fredrickson, B.F. Chmelka, G.D. Stucky, *Science* 279 (1998) 548.
- [3] P.T. Tanev, T.J. Pinnavaia, *Science* 271 (1996) 1267.
- [4] F. Kleitz, S.H. Choi, R. Ryoo, *Chem. Commun.* (2003) 2136.
- [5] A. Corma, *Chem. Rev.* 97 (1997) 2373.
- [6] J.S. Beck, J.C. Vartuli, W.J. Roth, M.E. Leonowicz, C.T. Kresge, K.D. Schmitt, C.T.-W. Chu, D.H. Olson, E.W. Sheppard, S.B. McCullen, J.B. Higgins, J.L. Schlenker, *J. Am. Chem. Soc.* 114 (1992) 10834.
- [7] L. Frunz, R. Prins, G.D. Pirngruber, *Microporous Mesoporous Mater.* 88 (2006) 152.
- [8] X. Chen, L. Huang, G. Ding, Q. Li, *Catal. Lett.* 44 (1997) 123.
- [9] A. Karlsson, M. Stöcker, R. Schmidt, *Microporous Mesoporous Mater.* 27 (1999) 181.
- [10] N. Petkov, M. Hözl, T.H. Metzger, S. Mintova, T. Bein, *J. Phys. Chem. B* 109 (2005) 4485.
- [11] Y. Liu, W. Zhang, T.J. Pinnavaia, *Angew. Chem. Int. Ed.* 40 (2001) 1255.
- [12] C. Madsen, C.J.H. Jacobsen, *Chem. Commun.* (1999) 673.
- [13] C.J.H. Jacobsen, C. Madsen, J. Houzvicka, I. Schmidt, A. Carlsson, *J. Am. Chem. Soc.* 122 (2000) 7116.
- [14] I. Schmidt, A. Boisen, E. Gustavsson, K. Stahl, S. Pehrson, S. Dahl, A. Carlsson, C.J.H. Jacobsen, *Chem. Mater.* 13 (2001) 4416.
- [15] H. Zhang, G.C. Hardy, Y.Z. Khimiyak, M.J. Rosseinsky, A.I. Cooper, *Chem. Mater.* 16 (2004) 4245.
- [16] M. Choi, D. Cho, R. Srivastava, C. Venkatesan, D.-H. Choi, R. Ryoo, *Nat. Mater.* 5 (2006) 718.
- [17] G.-T. Vuong, T.-O. Do, *J. Am. Chem. Soc.* 129 (2007) 3810.
- [18] H. Wang, T.J. Pinnavaia, *Angew. Chem. Int. Ed.* 45 (2006) 7603.
- [19] F.-S. Xiao, L. Wang, C. Yin, K. Lin, Y. Di, J. Li, R. Xu, D.S. Su, R. Schlögl, T. Yokoi, T. Tatsumi, *Angew. Chem. Int. Ed.* 45 (2006) 3090.
- [20] R. Srivastava, M. Choi, R. Ryoo, *Chem. Commun.* (2006) 4489.
- [21] H. Liu, X. Liu, X. Li, X. Xu, *Petrochem. Technol.* 27 (1998) X5.
- [22] S. Jun, R. Ryoo, *J. Catal.* 195 (2000) 237.
- [23] S. Che, K. Lund, T. Tatsumi, S. Iijima, S.H. Joo, R. Ryoo, O. Terasaki, *Angew. Chem. Int. Ed.* 42 (2003) 2182.
- [24] R.A. García, D.P. Serrano, D. Otero, *J. Anal. Appl. Pyrol.* 74 (2005) 379.

- [25] R. Ryoo, S.H. Joo, *Stud. Surf. Sci. Catal.* 148 (2004) 241.
- [26] A. Corma, V. Fornés, L. Forni, F. Márquez, J. Martínez-Triguero, D. Moscotti, *J. Catal.* 179 (1998) 451.
- [27] K.M. Keskinen, T.T. Pakkanen, P. Raulo, M. Ruotsalainen, P. Sarv, M. Titta, *Stud. Surf. Sci. Catal.* 84 (1994) 875.
- [28] R. Bertram, U. Lohse, W. Gessner, *Z. Anorg. Allg. Chem.* 567 (1988) 145.
- [29] J. Klinowski, *Prog. Nucl. Magn. Reson. Spectrosc.* 16 (1984) 237.
- [30] J. Jiao, S. Altwasser, W. Wang, J. Weitkamp, M. Hunger, *J. Phys. Chem. B* 108 (2004) 14305.
- [31] B.R. Germy, A. Pandurangan, *Appl. Catal. A Gen.* 295 (2005) 185.
- [32] S. Martens, A. Mithöfer, *Phytochemistry* 66 (2005) 2399.
- [33] M.C. Samolada, E. Grigoriadou, Z. Kiparissides, I.A. Vasalos, *J. Catal.* 152 (1995) 52.
- [34] J. Aguado, D.P. Serrano, M.D. Romero, J.M. Escola, *J. Chem. Soc. Chem. Commun.* (1996) 725.